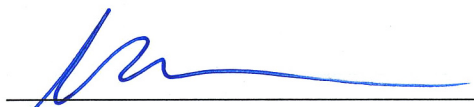


# Commissioning Data for Measurement of the Pixel Response Function and Focal Plane Geometry

KSCI-19100-001  
Stephen T. Bryson  
March 23, 2017

**NASA Ames Research Center**  
Moffett Field, CA 94035

Prepared by:  Date: March 23, 2017  
Stephen T. Bryson, Kepler Science Office

Approved by:  Date: March 23, 2017  
Michael R. Haas, Kepler Science Office Director

Approved by:  Date: March 23, 2017  
Natalie Batalha, Kepler Project Scientist

## Document Control

### Ownership

This document is part of the Kepler Project Documentation that is controlled by the Kepler Project Office, NASA/Ames Research Center, Moffett Field, California.

### Control Level

This document will be controlled under KPO @ Ames Configuration Management system. Changes to this document **shall** be controlled.

### Physical Location

The physical location of this document will be in the KPO @ Ames Data Center.

### Distribution Requests

To be placed on the distribution list for additional revisions of this document, please address your request to the Kepler Science Office:

Michael R. Haas  
Kepler Science Office Director  
MS 244-30  
NASA Ames Research Center  
Moffett Field, CA 94035-1000  
Michael.R.Haas@nasa.gov

The correct citation for this document is: S. T. Bryson, 2017, *Commissioning Data for Measurement of the Pixel Response Function and Focal Plane Geometry*, KSCI-19100-001

**Revision History:**

Date	Revision	Revision Description	Page(s)
3/23/17	KSCI-19100-001	Initial Release	

# Contents

<b>1</b>	<b>Introduction</b>	<b>6</b>
<b>2</b>	<b>Description of the Data</b>	<b>6</b>
	<b>Table 1: Observed Dither Offsets</b>	<b>11</b>

# 1 Introduction

This document describes the *Kepler* PRF/FPG data release. This data was taken on April 27-29, 2009, during *Kepler's* commissioning phase in order to measure the pixel response function (PRF) (Bryson et al., 2010a) and focal plane geometry (FPG) (Tenenbaum and Jenkins, 2010). 33,424 stellar targets were observed for 243 “long” cadences, each with a duration of 14.7 minutes (half the duration of a normal *Kepler* long cadence). During these 243 cadences the *Kepler* photometer was moved, pointing in a dither pattern to facilitate PRF measurement. Motion occurred during the even cadences (second, fourth, etc.), with the telescope in stable fine point at each pointing in the dither pattern during the odd cadences (first, third, etc.). The first and last cadences were at the center of the dither pattern. Motion cadences are included in this release, but they do not contain any data. For details on how this data was used to derive the *Kepler* PRF and FPG models, see Bryson et al. (2010a) and Tenenbaum and Jenkins (2010). Descriptions of the PRF and FPG models are found in Thompson et al. (2016), §2.3.5.17 and §2.3.5.16 respectively. The data in this release can be used to recompute the *Kepler* PRF and FPG. Such a reconstruction, however, would not reflect measured seasonal changes in the PRF described in Van Cleve et al. (2016b), §5.2.

The dither pattern is shown in Figure 1. The crosses show the commanded pointings and the circles show the measured pointings. Measured pointings are different from the commanded pointings due to the early state of calibration of the fine guidance sensors during commissioning (Van Cleve et al., 2016a). The measured offsets from the center of the pattern are given in RA/DEC offsets and pixel offsets in Table 1. The order of the offsets was randomized during data collection to avoid time-dependent systematics.

## 2 Description of the Data

The PRF/FPG data is released as 33,424 target pixel files, one for each stellar target, containing both raw and calibrated pixel data. The format of the data and the FITS headers are described in Thompson et al. (2016). There are no photometric light curves in this release. The target pixel files contain all 243 cadences, but due to the configuration of the *Kepler* processing pipeline, the in-motion (even) cadences contain all zeros. There are 122 non-motion (odd) cadences with non-zero data.

Each target pixel file includes an aperture extension, as described in Thompson et al. (2016), that provides the “optimal” photometric aperture for that target. In this data release, however, this aperture is not expected to be optimal because computing the optimal aperture requires knowledge of the PRF (Bryson et al., 2010b), which was unknown when this data was taken. Therefore the aperture is estimated, and the collected pixels are determined by that estimated aperture and three halos (Bryson et al., 2010b) that were added to assure that each target was full captured.

The data in this release was calibrated with the latest *Kepler* processing pipeline (SOC 9.3; Jenkins et al. (2017)), while the PRFs were computed during commissioning using the

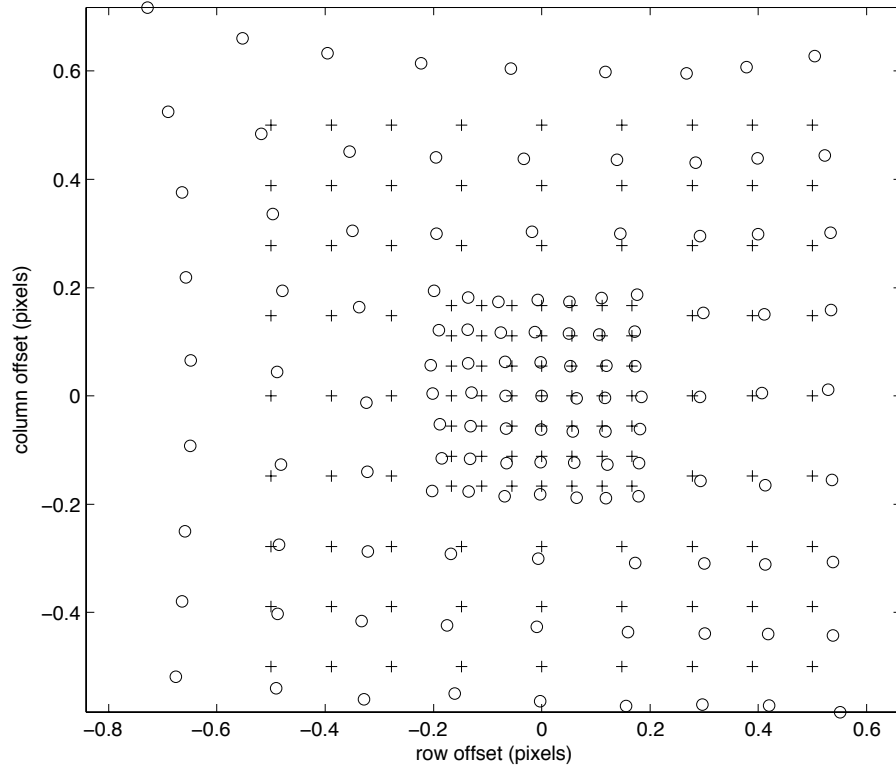


Figure 1: Commanded (+) and achieved (o) dither pattern used to measure the PRF. The discrepancy is due to the early state of calibration of the fine guidance sensors during commissioning.

SOC 5.0 version of the pipeline. Differences in pipeline processing lead to small differences between the calibrated pixels used to compute the PRFs during commissioning and the calibrated pixels in this release. Figure 2 shows the median and median absolute deviation of the relative difference between the two data sets for all 84 CCD channels. Most channels show an approximately 1% relative difference, with outliers as large as 5%. Figure 3 shows the prevalence of outliers in the relative difference of the two data sets for each channel. Specifically, Figure 3 shows the fraction of pixels that are brighter than twice the background value with differences between the original processing and this release greater than 10%. Most channels have less than 0.3% of their pixels being outliers, though channel 80 has 1% of its pixels being outliers. Essentially all the outliers in Figures 2 and 3 are due to improvements in the small-scale flat correction (Jenkins et al., 2017). This calibration change results in spurious flux in the apertures of a small number of targets originally used to compute the PRFs that is not present in this release. Because the number of effected targets is small, the impact of this spurious flux on the PRF computation during commissioning is inconsequential.



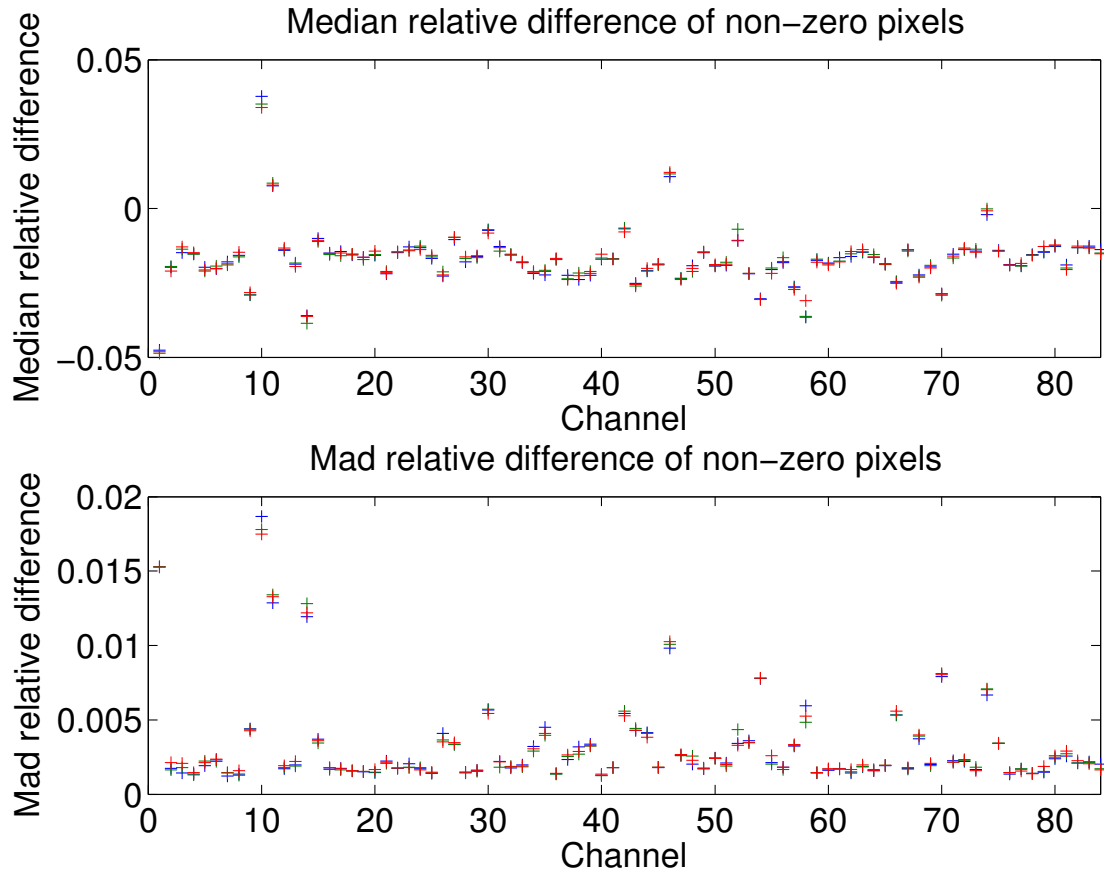


Figure 2: Statistics of the difference between the original PRF pixel data and this release by CCD channel for three of the 122 non-motion cadences. Top: median relative difference, showing a small median difference on all channels with outliers as large as 5%. Bottom: Median absolute relative deviation showing that the variation in the pixel values is very close with outliers less than 2%. Blue crosses: cadence 1. Green crosses: cadence 111. Red crosses: cadence 241.

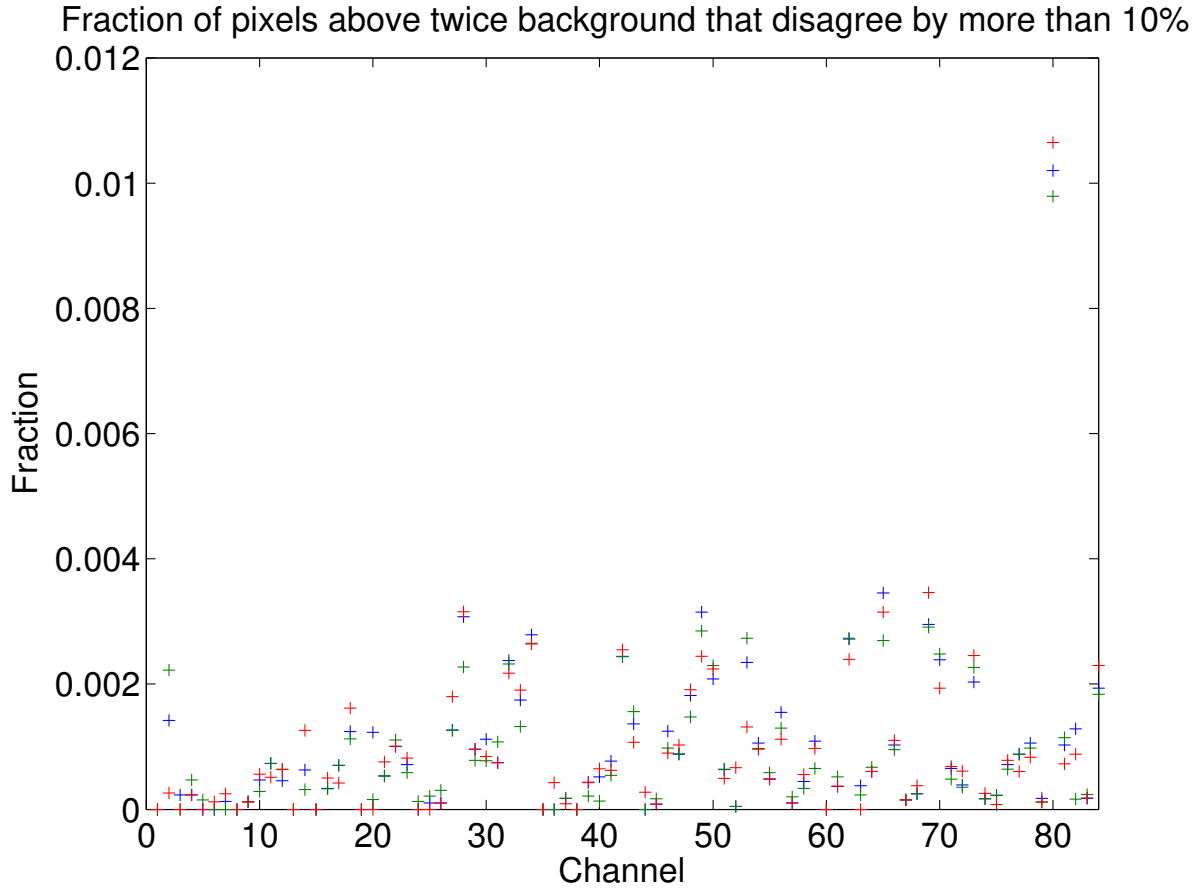


Figure 3: The fraction of those pixels brighter than twice the background that disagree between the original PRF data and this release by more than 10%, showing the prevalence of outlier pixels that are very different between the two data sets. Three of the 122 non-motion cadences are shown. Most channels have fewer than 0.3% of pixels being such outliers. Channel 80 has about 1% outlier pixels, which has been traced to errors in the original small-scale flat correction. Blue crosses: cadence 1. Green crosses: cadence 111. Red crosses: cadence 241.

Table 1: Observed Dither Offsets

Cadence	$\Delta$ RA (arcsec)	$\Delta$ DEC (arcsec)	$\Delta$ Row (pix)	$\Delta$ Column (pix)
1	0.00	0.01	0.00	0.00
3	1.22	2.25	0.30	0.57
5	0.36	0.81	0.12	0.19
7	-0.41	-0.28	-0.00	-0.12
9	-1.34	-2.70	-0.38	-0.65
11	0.32	-0.06	-0.06	0.06
13	2.22	0.67	-0.17	0.56
15	-3.33	0.26	0.51	-0.66
17	1.52	1.76	0.16	0.56
19	-1.78	1.47	0.55	-0.17
21	1.09	1.48	0.16	0.43
23	-0.67	2.22	0.56	0.17
25	1.78	0.40	-0.16	0.43
27	-0.26	0.40	0.12	0.00
29	0.64	-2.51	-0.61	-0.21
31	-0.59	0.46	0.18	-0.06
33	-0.86	-2.21	-0.35	-0.48
35	-0.38	1.79	0.43	0.17
37	0.25	-0.40	-0.12	-0.00
39	2.55	0.16	-0.32	0.56
41	0.36	-1.91	-0.45	-0.19
43	0.51	2.38	0.43	0.44
45	-0.33	-3.39	-0.67	-0.54
47	-0.11	1.37	0.30	0.17
49	0.13	-2.93	-0.63	-0.38
51	-0.23	-1.04	-0.19	-0.19
53	-0.53	-0.09	0.05	-0.12
55	-1.99	0.66	0.41	-0.33
57	0.53	0.06	-0.06	0.12
59	0.99	-0.21	-0.18	0.18
61	0.66	3.12	0.57	0.57
63	-0.12	0.19	0.06	-0.00
65	-2.70	-0.59	0.25	-0.65
67	0.65	-1.06	-0.31	-0.01
69	-1.16	-1.69	-0.19	-0.48
71	-0.80	0.31	0.18	-0.13
73	1.20	-2.13	-0.61	-0.04
75	-2.78	0.71	0.53	-0.49
77	0.08	0.33	0.06	0.06

Table 1: Observed Dither Offsets

Cadence	$\Delta$ RA (arcsec)	$\Delta$ DEC (arcsec)	$\Delta$ Row (pix)	$\Delta$ Column (pix)
79	-2.29	1.08	0.54	-0.33
81	-1.22	1.85	0.56	-0.00
83	-0.05	0.53	0.12	0.06
85	-1.48	1.03	0.42	-0.17
87	1.19	-0.69	-0.31	0.16
89	-1.85	-0.59	0.13	-0.47
91	-1.39	-0.22	0.15	-0.32
93	0.91	-1.52	-0.45	-0.02
95	1.96	-0.86	-0.45	0.29
97	1.67	-0.38	-0.31	0.30
99	0.02	0.87	0.18	0.12
101	0.37	1.69	0.30	0.31
103	-0.03	-0.89	-0.18	-0.13
105	0.74	0.21	-0.06	0.18
107	0.66	-0.12	-0.12	0.12
109	-1.71	0.25	0.29	-0.32
111	0.22	2.82	0.56	0.44
113	-0.33	0.07	0.06	-0.06
115	-0.16	-0.68	-0.12	-0.13
117	0.10	2.11	0.43	0.31
119	3.19	-0.97	-0.64	0.54
121	0.40	0.28	0.00	0.12
123	1.43	0.94	0.00	0.43
125	-1.20	0.62	0.30	-0.17
127	-1.65	-2.14	-0.22	-0.64
129	0.28	0.47	0.06	0.12
131	-1.05	-0.74	-0.01	-0.32
133	-1.08	-3.26	-0.54	-0.68
135	-0.37	-0.83	-0.12	-0.19
137	0.86	0.01	-0.12	0.18
139	-0.88	-0.03	0.11	-0.19
141	-0.75	-0.23	0.06	-0.19
143	0.78	-0.34	-0.18	0.12
145	1.76	-1.75	-0.61	0.13
147	2.38	-0.61	-0.46	0.42
149	-0.46	0.26	0.12	-0.06
151	1.46	-1.16	-0.45	0.15
153	2.84	-0.34	-0.46	0.55
155	-2.00	-1.58	-0.06	-0.64

Table 1: Observed Dither Offsets

Cadence	$\Delta$ RA (arcsec)	$\Delta$ DEC (arcsec)	$\Delta$ Row (pix)	$\Delta$ Column (pix)
157	-0.14	-2.30	-0.46	-0.35
159	-0.18	0.73	0.18	0.06
161	0.12	-0.19	-0.06	-0.00
163	1.87	1.22	-0.00	0.56
165	-0.41	-1.80	-0.32	-0.33
167	-0.67	0.12	0.12	-0.13
169	-2.36	-1.05	0.10	-0.64
171	-0.20	2.54	0.56	0.31
173	-0.08	-0.33	-0.06	-0.06
175	0.38	-0.60	-0.18	-0.00
177	1.36	0.13	-0.16	0.30
179	0.60	0.42	0.00	0.18
181	-3.00	-0.17	0.38	-0.65
183	-0.29	-0.47	-0.06	-0.13
185	-0.21	-0.13	0.00	-0.06
187	-0.39	0.60	0.18	0.00
189	2.70	-1.21	-0.63	0.40
191	0.22	1.01	0.18	0.18
193	-0.66	1.01	0.30	0.00
195	-0.50	-0.62	-0.06	-0.19
197	1.01	0.68	0.00	0.31
199	0.67	1.21	0.16	0.31
201	2.26	-1.45	-0.62	0.28
203	-0.93	1.42	0.43	-0.00
205	-0.62	-0.42	-0.00	-0.19
207	-0.84	-3.99	-0.72	-0.73
209	0.45	-0.26	-0.12	0.06
211	0.92	2.67	0.43	0.56
213	0.17	-0.74	-0.18	-0.07
215	0.04	-0.53	-0.12	-0.07
217	-1.02	0.17	0.18	-0.19
219	0.57	-0.47	-0.18	0.06
221	-2.18	-0.12	0.27	-0.48
223	0.47	0.61	0.06	0.18
225	-0.72	-1.29	-0.17	-0.33
227	-2.48	0.29	0.40	-0.48
229	0.14	0.67	0.12	0.12
231	2.09	-0.12	-0.31	0.42
233	0.77	1.95	0.30	0.43

Table 1: Observed Dither Offsets

Cadence	$\Delta$ RA (arcsec)	$\Delta$ DEC (arcsec)	$\Delta$ Row (pix)	$\Delta$ Column (pix)
235	-1.51	-1.13	-0.03	-0.47
237	0.08	-1.43	-0.31	-0.18
239	0.19	0.13	0.00	0.06
241	-0.61	-2.75	-0.49	-0.51
243	-0.01	0.00	0.00	-0.00

## References

Bryson, S. T., et al. 2010a, ApJ 713, L97

Bryson, S. T., et al. 2010b, Proc. SPIE 7740, 77401D

Jenkins, J., et al. 2017, *Kepler Data Processing Handbook*, KSCI-19081-002

Tenenbaum, P. and Jenkins, J. M., 2010, *Proc. SPIE 7740 77401C*

Thompson, S., et al. 2016, *Kepler Archive Manual*, KSCI-19008-006

Van Cleve, J., et al. 2016a, *Kepler Instrument Handbook*, KSCI-19033-002

Van Cleve, J., et al. 2016b, *Kepler Data Characteristics Handbook*, KSCI-19040-005